Biogeosciences Discuss., 11, 15549–15584, 2014
www.biogeosciences-discuss.net/11/15549/2014/
doi:10.5194/bgd-11-15549-2014

Biogeosciences Discussions
Open Access

Trends and drivers in global surface ocean pH over the past three decades

S. K. Lauvset[1,2], N. Gruber[3], P. Landschützer[3], A. Olsen[1,2,4], and J. Tjiputra[2,4]

[1]Geophysical Institute, University of Bergen, Bergen, Norway
[2]Bjerknes Center for Climate Research, Bergen, Bergen, Norway
[3]Environmental Physics, Institute of Biogeochemistry and Pollutant Dynamics, ETH Zurich, Zürich, Switzerland
[4]Uni Climate – Uni Research, Bergen, Norway

Received: 5 October 2014 – Accepted: 13 October 2014 – Published: 7 November 2014

Correspondence to: S. K. Lauvset (siv.lauvset@gfi.uib.no)

Published by Copernicus Publications on behalf of the European Geosciences Union.

Abstract

We report global long-term trends in surface ocean pH using a new pH data set computed by combining fCO_2 observations from the Surface Ocean CO_2 Atlas (SOCAT) version 2 with surface alkalinity estimates based on temperature and salinity. Trends were determined over the periods 1981–2011 and 1991–2011 for a set of 17 biomes using a weighted linear least squares method. We observe significant decreases in surface ocean pH in ∼ 70 % of all biomes and a global mean rate of decrease of $-0.0018 \pm 0.0004\,yr^{-1}$ for 1991–2011. We are not able to calculate a global trend for 1981–2011 because too few biomes have enough data for this. In two-thirds of the biomes, the rate of change is commensurate with the trends expected based on the assumption that the surface ocean pH change is only driven by the surface ocean carbon chemistry remaining in a transient equilibrium with the increase in atmospheric CO_2. In the remaining biomes deviations from such equilibrium may reflect changes in the trend of surface ocean fCO_2, most notably in the equatorial Pacific Ocean, or changes in the oceanic buffer (Revelle) factor. We conclude that well-planned and long-term sustained observational networks are key to reliably document the ongoing and future changes in ocean carbon chemistry due to anthropogenic forcing.

1 Introduction

The concentration of atmospheric carbon dioxide (CO_2) is rapidly increasing due to the burning of fossil fuels, cement production, and land use changes (Le Quéré et al., 2014). This drives a net flux of CO_2 into the ocean, causing its concentration of CO_2 to increase, which drives a decrease in pH and in the concentration of the carbonate ion (CO_3^{2-}, Doney et al., 2009b; Zeebe and Wolf-Gladrow, 2001). These changes in the chemistry of the oceanic carbonate system, collectively referred to as ocean acidification (Gattuso and Hansson, 2011), are a source of concern due to their potential impact on organisms, ecosystems and biogeochemical cycles (Doney et al.,

Discussion Paper | Discussion Paper | Discussion Paper | Discussion Paper |

BGD
11, 15549–15584, 2014

Trends and drivers in global surface ocean pH over the past three decades

S. K. Lauvset et al.

2009a). But in contrast to the surface ocean fugacity of carbon dioxide (fCO_2), for which many studies have analyzed the long-term trends, both regionally and globally (e.g. Fay and McKinley, 2013; Le Quéré, 2010; Lenton et al., 2012; Takahashi et al., 2009b), only a handful of regional studies have so far been published on long-term pH trends (Bates, 2007; Dore et al., 2009; Gonzalez-Davila et al., 2007; Olafsson et al., 2010).

The most extensive assessment to date is the one of Bates et al. (2014). They described changes in ocean carbon cycle variables at seven time-series stations, all of which have been occupied for at least two decades. Their analysis shows that while there are regional differences, these open ocean time-series show remarkably similar trends in dissolved inorganic carbon (DIC), fCO_2, and pH. At the tropical and subtropical open ocean stations (Bates, 2007; Dore et al., 2009; Gonzalez-Davila et al., 2010) ocean pH is decreasing at a rate of $-0.0017 \pm 0.0002\,\text{yr}^{-1}$. At the high-latitude stations, however, a more variable picture emerges. While the pH trend in the Icelandic Sea follows the rate observed at the lower latitude stations, the trend in the Irminger Sea (Olafsson et al., 2010) is nearly twice as large, i.e., $-0.0026 \pm 0.0006\,\text{yr}^{-1}$. Thus, in a global analysis, we expect a complex spatial pattern of long-term trends, yet hitherto unknown.

The absence of a global analysis of long-term trends is largely a consequence of the lack of direct surface ocean pH measurements, which is in sharp contrast to the situation for surface ocean fCO_2, for which data products contain several million observations (Bakker et al., 2014; Pfeil et al., 2013; Takahashi et al., 2009a). This limitation can be overcome by using computed pH, obtained by combining the very large data products of fCO_2 with estimates of surface alkalinity. Lauvset and Gruber (2014) demonstrated for the North Atlantic that this approach is able to produce rather accurate estimates of surface ocean pH. Takahashi et al. (2014) came to the same result globally. This is largely because variations in pH are mostly driven by variations in DIC following CO_2 uptake, and only to a lesser degree by variations in alkalinity. Thus, uncertainties and errors in the alkalinity estimated from salinity and temperature

BGD
11, 15549–15584, 2014

observations have only a limited effect on the uncertainties and error of the computed pH (Lauvset and Gruber, 2014).

Even though the use of pH computed from fCO_2 generates a global data set containing millions of pH observations, the resulting data are still sparse in time and space on a global scale, making the determination of global long-term trends challenging. For surface pCO_2 this challenge has historically been overcome by binning the data into a very coarse grid (order of 5–10° in latitude and longitude) by e.g. Lenton et al. (2012) and Takahashi et al. (2002, 2009b), but more recently Fay and McKinley (2013) proposed to aggregate the data into biomes. This type of aggregation is more likely to capture the correct long-term dynamics of a region, as one expects a biome to respond in a more coherent manner to perturbations than a region defined by a latitude/longitude range.

Given the absence of a global observation-based analysis of pH trends, models have so far been the only source of information. The Norwegian Earth System Model (NorESM1-ME), as part of the Coupled Model Intercomparison Project phase 5 (CMIP5, Taylor et al., 2012), simulates a global average pH decrease of $-0.0017\,yr^{-1}$ (1981–2011), which is largely commensurate with observations reported from the time series stations. A recent study using ten different CMIP5 models, including NorESM1-ME, showed that all models give similar global average pH trends – both in the historical and future scenarios (Bopp et al., 2013).

This secular pH trend of $-0.0017\,yr^{-1}$ and the low spread between models is expected for an ocean where (i) the surface ocean fCO_2 follows that in the atmosphere due to the sufficiently rapid exchange of the excess CO_2 between the atmosphere and the surface ocean, and (ii) where the buffer (Revelle) factor remains spatially uniform and close to constant, as the partial derivative $\partial[H^+]/\partial fCO_2$ is directly related to this quantity (Orr, 2011; Sarmiento and Gruber, 2006). While the latter may be a good assumption for the global average, this may not be the case regionally and locally, where most of the impacts of ocean acidification will occur. Bates et al. (2014) show, for example, not only variations between the high- and low latitude secular trends,

BGD
11, 15549–15584, 2014

but also that the Revelle factor is increasing at all time-series stations. This causes a decrease in the buffer capacity and hence a faster increase in surface ocean pH for a given increase in surface fCO_2 from the addition of CO_2. This trend in the Revelle factor is expected as much of the CO_2 newly added to the surface ocean from the atmosphere will be titrated away by CO_3^{2-} causing a decrease in its concentration. This decreases the ability of the surface ocean to "buffer" the pH against further uptake of CO_2, thus increasing the Revelle factor (Sarmiento and Gruber, 2006). But there are also other factors influencing the Revelle factor, mainly those processes that affect DIC and alkalinity, such as changes in ocean productivity and calcification, while changes in temperature and salinity are of minor importance (Sarmiento and Gruber, 2006).

Thus local and regional changes in the buffer factor have the potential to substantially decouple the pH trends from those of the surface ocean fCO_2, potentially causing a more variable pattern in the pH trends. The complex spatial variability, identified by Bates et al. (2014) and others (e.g. Tjiputra et al., 2014) support this hypothesis. This also shows that analyses of global pH trends are required for a comprehensive picture, including the regional distribution of changes and the dynamics of the changing ocean carbon system. Global analyses are also necessary for the validation of model results, for underpinning and interpreting response studies from organism to ecosystem level, and for optimizing the planning of continued and future observational networks.

Here we take advantage of the approach of Lauvset and Gruber (2014) to determine global ocean pH trends, and their drivers, using pH data calculated from the more than 10 million observations of surface ocean fCO_2 that have been made available through the Surface Ocean CO_2 Atlas (SOCAT) project (Bakker et al., 2014; Pfeil et al., 2013). Although pH is the main parameter of our study fCO_2 has been carried through all of our analyses in order to determine how effects of carbonate chemistry variations causes the evolution of pH to differ from that expected from fCO_2 alone in many regions. Finally we use the long term pH trends derived from a global earth system model, the NorESM1-ME, in order to illustrate how important spatial variability is for the representativeness of our trend results.

BGD
11, 15549–15584, 2014

2 Data and methods

We calculated pH in the surface ocean by a two-step calculation using observations of fCO_2, sea surface temperature (SST), and sea surface salinity (SSS) from SOCAT version 2, (Bakker et al., 2014). In the first step, alkalinity was calculated from SSS and SST using the algorithms developed by Lee et al. (2006) and Nondal et al. (2009). The Nondal et al. (2009) algorithms were developed specifically for the high-latitude (> 60° N) Atlantic Ocean, and were used only there. Whenever no measured SSS was available in the SOCATv2 data set the climatological World Ocean Atlas SSS value (Antonov et al., 2010) – which is included in the SOCATv2 data product – was used instead. The SOCAT SSS data have not been quality controlled and might therefore be biased. Lauvset and Gruber (2014) showed that this potential bias does not greatly affect the precision of the pH trends. It may affect the accuracy of the calculation but for our purpose of determining long-term trends the accuracy (i.e. the lack of bias in the data) is of less importance as long as the precision is good enough, and assuming that any bias remains constant over time. In the second step, pH on the total scale at in situ temperature was calculated from the estimated alkalinity and the observed fCO_2 using CO2SYS (Lewis and Wallace, 1998). We used the K_1 and K_2 constants from Mehrbach et al. (1973) refit by Dickson and Millero (1987), and the borate to salinity ratio from Uppström (1974). Since we use CO2SYS this calculation also gives us dissolved inorganic carbon (DIC) and all other variables of the ocean carbon chemistry system.

Quite a few of the data fall outside the valid ranges for input data for the Lee et al. (2006) and Nondal et al. (2009) alkalinity algorithms and are lost in this step. There remains 7 381 013 data points of pH (and alkalinity) over the global ocean in the time period 1973–2011. The global calculation error (precision) for pH is 0.0032 ± 0.0005, and the calculated pH compares well to observed pH at crossover locations in the Atlantic Ocean (Lauvset and Gruber, 2014). Before analysis the pH data were bin averaged into monthly $1^\circ \times 1^\circ$ bins, using no extrapolation or interpolation

BGD
11, 15549–15584, 2014

of the data. The global data set was divided into the 17 ocean biomes defined and named by Fay and McKinley (2014) as shown in Fig. 1. Here, we only evaluate trends in the open ocean, and data from coastal regions shallower than 250 m, based on the ETOPO2 bathymetry and those with salinity < 20 were removed.

In each biome a least squares linear regression weighted with Tukey's bisquare method was used to determine the long-term pH trend. For the long-term trend determination we required each biome to have at least three observations in each decade (1981–1990, 1991–2000, and 2001–2011). While this criterion was met in only 8 biomes for the period 1981–2011, all 15 had sufficient data for the period 1991–2011. Both ordinary and weighted least squares regressions were carried out, but we chose a weighted least squares regression over an ordinary least squares regression since this is less sensitive to outliers in the data. This makes the statistics of the regression more robust, but generally this choice does not significantly affect the results presented here. All regression results are presented with the standard error of the slope (se), which represents its 68 % confidence interval, and the root mean square error (RMSE). The RMSE is used as a measure of interannual variability.

Before the regression analysis was carried out two corrections were applied to the data: deseasonalization and removal of spatial bias. The importance of these corrections, particularly in data sparse biomes such as those in the Southern Ocean, was recently highlighted by Fay et al. (2014). The seasonal cycle in the data was removed following Takahashi et al. (2009b), using the long-term average seasonal cycle as contained in our data for each biome for this correction. However, we find that using the climatological seasonal cycle – calculated using the Takahashi $p\mathrm{CO_2}$ climatology (Takahashi et al., 2009a) – do not significantly affect the results. To correct for any spatial bias in the large scale biomes the difference between the climatological value in each $1^\circ \times 1^\circ$ bin and the biome mean climatological value was subtracted from the observed value in each $1^\circ \times 1^\circ$ bin. There is no difference between this method and simply subtracting the climatological value in each $1^\circ \times 1^\circ$ bin, but our approach retains the biome mean values. It should be noted that the computed trends in some

BGD
11, 15549–15584, 2014

biomes are sensitive to which climatological data is used for the spatial bias correction: subtracting the climatological value vs. subtracting the long-term average in each $1^{\circ} \times 1^{\circ}$ bin. Mostly this is because in some $1^{\circ} \times 1^{\circ}$ bins, the long-term average is biased towards the last decade, which has significantly more data than earlier periods.

A statistical test was performed to ensure that the effects of these corrections do not corrupt our analysis: results after applying one or both corrections were compared to results after applying none using a one-way analysis of variance (ANOVA, see e.g. Vijayvargiya, 2009). The deseasonalization removes scatter in the data and leads to more robust regressions, but does not significantly (p value < 0.05) affect the long-term trend in any biome or time period. The spatial bias correction has in most biomes no statistically significant impact on the long-term trend, but because it does affect the trend in some biomes we decided to keep it applied. The long-term pH trend is also much more sensitive to this correction than the fCO_2 trend, mostly because the pH trend is very small and thus more sensitive to any data correction.

The pH change expected from a certain change in fCO_2 assuming everything else (i.e. alkalinity, DIC, SST, Revelle factor) remains constant was calculated using $\Delta pH/\Delta fCO_2 = \partial pH/\partial fCO_2$. The partial derivative was estimated in CO2SYS using 0.01 µatm increments in fCO_2. We used the same equation to evaluate what global average fCO_2 change the global long-term trend in pH is consistent with, but then using -0.001 incremental changes in pH. Using such small increments allowed us to abide by the assumption of constant DIC and Revelle factor.

In each biome the long-term trend in pH was decomposed into the effects of changes in SST, SSS, alkalinity, and DIC. First the impact of each of these drivers on the fCO_2 trend was determined following Takahashi et al. (1993), Eqs. (2)–(5), we then converted our results to the impacts on $[CO_2]$ and on $[H^+]$ following Eq. (1.5.87) in Zeebe and Wolf-Gladrow (2001), and finally we determined the impact on pH. The DIC data and dissociation constants required for these calculations were calculated in CO2SYS from the fCO_2 and alkalinity pair in the same calculation that gave us pH.

BGD
11, 15549–15584, 2014

To test whether, and how the highly variable spatial and temporal coverage of the observational data affect the results we have used the NorESM1-ME Earth system model, which prognostically simulates the seawater carbon chemistry. A detailed description and evaluation of the model simulation is available in Tjiputra et al. (2013). We examined the model simulation for the 1981–2011 period based on the CMIP5 historical and future RCP8.5 scenarios, where the atmospheric CO_2 concentration is used as the boundary condition. We binned the model monthly output into the same $1^\circ \times 1^\circ$ bins and used the same method to calculate and decompose the long-term trends in each biome as we used for the observational data – including the two-step pH calculation described above. Two sets of model trends were determined. For the first, we used the fully sampled model output, referred to here as the "fully-sampled trend". For the second set, we subsampled the model output following the observational coverage, i.e. only data from monthly grid cells corresponding to those where real observations have been obtained were used. The "sub-sampled trend" was then computed from these subsampled model data. The comparison of these two informs us on how sensitive the calculated trends are to the variable data coverage.

3 Results and discussion

3.1 Long-term trends in pH

We find statistically significant trends in 6 out of the 8 biomes with sufficient data for the period 1981–2011, and for 13 out of the 15 biomes with sufficient data for the period 1991–2011 (Fig. 1 with the numerical values in Table 1). As shown in Figs. 2–4, the data coverage in each biome is generally very good after 1990, but often spotty prior to this year. These figures also reveal a substantial amount of interannual variability around the determined trends, with RMSE values of between 0.01 and 0.04 pH units – i.e., roughly of similar magnitude as the cumulative trend over the 20–30 years of analyses. No robust analyses were possible for the North Pacific ice covered (NP-ICE) and North

BGD
11, 15549–15584, 2014

Atlantic ice covered (NA-ICE) biomes, due to the lack of data (< 20 data points) hence they are not further discussed in the paper. Unfortunately, these are the Arctic biomes where the earliest impacts of ocean acidification are expected (Steinacher et al., 2009).

The regions with sufficient data, but without statistically significant trends, i.e., the North Pacific subpolar seasonally stratified (NP-SPSS) biome for the period 1981–2011, and the Southern Ocean subtropical seasonally stratified (SO-STSS) and ice covered (SO-ICE) biomes for the period 1991–2011, are characterized by large RMSE and a substantial amount of decadal variability, which is likely masking the long-term trends. In addition to these three biomes where the trends are statistically indistinguishable from zero, the South Pacific subtropical permanently stratified (SP-STPS) biome is likely biased by its low data density, and will not be further discussed. This decision was corroborated was by comparing the pH trend in the fully-sampled model results with the sub-sampled model results (Fig. 5): the SP-STPS biome is the only one where the difference in these trends is statistically significant at the 95 % confidence level.

The area-weighted global average pH decrease, including only statistically significant trends, is $-0.0018 \pm 0.0004\,\mathrm{yr}^{-1}$ for the period 1991–2011. No global trend can be computed for the 1981–2011 period, as the number of biomes with trend estimates is too small, but the Pacific Ocean trend in this period is $-0.0019 \pm 0.0001\,\mathrm{yr}^{-1}$. Within the uncertainty limits the global 1991–2011 trend is comparable to the global trend in the fully-sampled NorESM1-ME model results ($-0.0017\,\mathrm{yr}^{-1}$) and to the average trend of $-0.0018 \pm 0.0003\,\mathrm{yr}^{-1}$ over the seven time series evaluated by Bates et al. (2014). Assuming that everything, including the Revelle factor, remains constant, this global average pH trend corresponds to a rate of increase in surface ocean $f\mathrm{CO_2}$ of $1.75 \pm 0.4\,\mathrm{\mu atm\,yr}^{-1}$, which is roughly the rate of increase in atmospheric $p\mathrm{CO_2}$. Regionally, however, the response of the ocean carbon system to the atmospheric forcing is more variable (Fig. 1).

In the North Atlantic subpolar seasonally stratified (NA-SPSS) biome the observed pH trend is $-0.0020 \pm 0.0004\,\mathrm{yr}^{-1}$. This is right in between the trend observed at the

BGD
11, 15549–15584, 2014

Irminger Sea time series ($-0.0026 \pm 0.0006\,yr^{-1}$) and that observed at the Iceland Sea time series ($-0.0014 \pm 0.0005\,yr^{-1}$) (Bates et al., 2014). But within the 68 % confidence intervals, the NA-SPSS pH trend is consistent with both of these local trends. In the North Atlantic subtropical seasonally stratified (NA-STSS) biome there are no time series data to compare with, but its trend of $-0.0018 \pm 0.0003\,yr^{-1}$ is consistent with a trend of $\sim -0.0020\,yr^{-1}$ observed in the Rockall Trough by McGrath et al. (2012). In the North (NA-STPS) and South (SA-STPS) Atlantic subtropical permanently stratified biomes the pH trend is the same, but the RMSE values indicate larger interannual variability in the southern biome (Table 1). The trend identified here for the NA-STPS ($-0.0011 \pm 0.0002\,yr^{-1}$) is significantly lower than the trend observed at the Bermuda Atlantic Time-series Study (BATS, Bates et al., 2014), of $-0.0017 \pm 0.0001\,yr^{-1}$. Unfortunately, we have no time series data for comparison in the SA-STPS biome. In the Atlantic Ocean equatorial region (A-EQU) the pH trend ($-0.0016 \pm 0.0003\,yr^{-1}$) is lower than that observed at the Carbon Retention in A Colored Ocean (CARIOCA) time-series station of $-0.0025 \pm 0.0004\,yr^{-1}$ (Bates et al., 2014), but this station is located at the very edge of the biome in a more coastal setting and not ideal for comparison.

In the Pacific Ocean the RMSE around the fitted pH trends is generally larger than in the Atlantic Ocean (Table 1), possibly reflecting the higher interannual variability of the surface carbonate system there (see e.g., Landschützer et al. (2014) for $p\mathrm{CO_2}$ variability). In the North Pacific subtropical permanently stratified (NP-STPS) biome the pH trend of $-0.0016 \pm 0.0002\,yr^{-1}$ is the same as that observed at the Hawaii Ocean Time-series (HOT, Bates et al., 2014). The trends in the two equatorial Pacific Ocean biomes differ substantially. While the western biome (WP-EQU) has a relatively weak trend ($-0.0010 \pm 0.0002\,yr^{-1}$), the eastern (EP-EQU) biome has a much stronger pH trend than any other biome except the IO-STPS. This could be related to the recent trend toward stronger and more prevalent La Niña conditions in the eastern tropical Pacific leading to stronger upwelling, and higher surface $f\mathrm{CO_2}$ and lower pH in this region (Rödenbeck et al., 2014).

BGD
11, 15549–15584, 2014

The Indian Ocean subtropical permanently stratified (IO-STPS) biome had a very strong pH trend the past 30 years, only rivaled by that in the EP-EQU biome, as mentioned above. There are not any time series stations in the Indian Ocean to compare with, but fCO_2 trends for the Indian Ocean computed by Metzl (2009) are considerably larger than what we find: 2.11 µatm yr^{-1} vs. 1.44 ± 0.24 µatm yr^{-1}. Hence there is no reason to believe that our approach overestimates the pH trends here. In the Southern Ocean only the subpolar seasonally stratified (SO-SPSS) biome has a statistically significant pH trend, which at -0.0020 ± 0.0002 yr^{-1} is comparable to that in the NA-SPSS biome. Further, this trend is very similar to that calculated for this region by Takahashi et al. (2014), although they had used a different method.

3.2 Effects of changes in carbonate chemistry

To first order, the pH trends are expected to represent the direct response to increasing oceanic CO_2, as is the case for the long-term trends in surface ocean fCO_2. In order to assess how our results compare against this expectation, we have calculated two expected pH rates of change: first the 1981–2011 change in pH resulting from a surface ocean fCO_2 rate of change equal to that in the atmosphere (1.8 ± 0.1 µatm yr^{-1}) while keeping all other variables constant at their 1981 values; and second the change in pH that would be expected if the pH change mirrored the observed fCO_2 change in each biome provided that all other variables were kept at their 1981 values. The first expected pH change reflects how pH should change if the change in atmospheric CO_2 was the sole driver for the change in ocean pH. The second expected pH change reflects how pH should change if the oceanic fCO_2 changes were allowed to depart from the atmospheric ones but fCO_2 change remaining the only driver of pH change. Given our method of calculation (Sect. 2), both expected pH estimates assumes constant buffer (Revelle) factor.

Figure 6 shows both expected pH changes along with the observed pH change in each biome. Only the 13 biomes that have statistically significant pH trends for either 1981–2011 or 1991–2011 (Fig. 1) are discussed further. When the atmospheric CO_2

BGD
11, 15549–15584, 2014

increase is assumed to be the only driver for the pH changes, we find that in 5 of the 12 biomes the observed pH trends significantly differ from the expected pH change. This is due either to the uncertainty in the observed trends, to associated changes in carbonate chemistry, or to the surface ocean fCO_2 trends being significantly different from that in the atmosphere. However, the observed pH trends significantly differ from the expected pH change calculated using the observed fCO_2 trend in 5 of the 12 biomes also (Fig. 6). Only 3 of the 5 biomes are the same in both cases. Thus, the surface ocean fCO_2 trend not exactly mirroring the atmospheric cannot explain the discrepancy between expected and observed pH trends in most biomes. It may be an explanation in the equatorial Pacific biomes (EP-EQU and WP-EQU) where there is no discrepancy between observed and expected pH trends when the observed fCO_2 trend is used to calculate the expected pH change (Fig. 6), but a significant difference when an atmospheric rate of change is assumed.

The observed pH trend is more often smaller than that expected for the ocean mirroring the atmospheric fCO_2 change than vice versa. Only the EP-EQU biome has an observed pH change larger than the expected (Fig. 6). In the biomes where the observed trend differs from the expected trend there are indications which point to changes in carbonate chemistry, e.g. that the temporal trends in both $\partial[H^+]/\partial pCO_2$ (Gattuso and Hansson, 2011) and Revelle factor are consistent with the differences between expected and observed pH change. However, given the combined calculation errors, generally high level of noise in our data, and relatively few data points, only some of these indications are statistically significant. Further analysis of these spatial patterns needs to be undertaken using independent pH data, preferably direct measurements in order to quantify any possible biases in the results due to our pH being a calculated variable. A combination of SOCAT data with repeat hydrography and time-series data would be ideal but this is outside the scope of this study.

BGD
11, 15549–15584, 2014

Title Page
Abstract | Introduction
Conclusions | References
Tables | Figures
◀| |▶
◀ ▶
Back | Close
Full Screen / Esc
Printer-friendly Version
Interactive Discussion

3.3 Major driving forces behind the observed pH and trends

The decomposition of the fCO_2 and pH trends confirms (Figs. 8–10) that in all biomes the long-term increase in DIC is by far the dominant driver for the long-term pH changes. Thus, knowledge about the changes in ocean DIC therefore is the most important in understanding – and predicting – changes in ocean pH (Table 2). This is not unexpected since the open ocean is in – or very close to – chemical equilibrium with the atmosphere (Lauvset and Gruber, 2014). Thus the surface ocean is taking up CO_2 from the atmosphere in order to re-establish a chemical equilibrium, leading to a corresponding increase in pCO_2 and DIC. It must be noted that since we do not have measurements of alkalinity this parameter is calculated from SST and SSS, and the relatively large uncertainties in these calculations may add a degree of uncertainty to the decomposition. Due to a lack of independent data this is not further evaluated in this study.

In the Atlantic Ocean biomes the second most important driver is SST (Fig. 8), which mostly has a positive change and therefore has limited the DIC increase required to maintain an fCO_2 growth rate similar to that in the atmosphere. SST is the second most important driver also in the Pacific Ocean biomes (Fig. 9), but here SST decreased in many biomes leading to an enhanced increase in DIC through uptake from the atmosphere. In the Southern Ocean biomes alkalinity changes have a significant impact on the trends (Fig. 10), which also modulates the DIC changes. Decreasing alkalinity over time increases fCO_2 so that the DIC change required to maintain a sea surface fCO_2 growth rate similar to the atmospheric is reduced.

In most biomes there is a residual between the sum of the four components and the observed trend (Fig. 7). Lenton et al. (2012) performed a similar analysis and attributed such residuals to the use of a spatial mean Revelle factor, the approximations underlying the Takahashi et al. (1993) equations, and the assumption of linear trends in all variables. We tested whether variable data coverage is also an important contributor to this residual by subsampling the NorESM1-ME simulated pH data and comparing the resulting 1981–2011 decomposition with the decomposition determined using the full model output. Figure 7 illustrates that in most biomes there are similar residuals between the sum of the four components and the actual trends in the sub-sampled and fully-sampled model fields as well. We can, therefore, find no evidence to show that poor data coverage is of major importance in determining what drives the change in surface ocean pH.

3.4 Recent changes in the Southern Ocean biomes

While this study generally does not have statistically significant results in the Southern Ocean our results do indicate significant decadal variations in the trends (Table 1). This is consistent with the changing fCO_2 trends in a recent study by Fay et al. (2014) as well as previous findings of a change in the CO_2 sink in this region (e.g. Fay and McKinley, 2013; Landschützer et al., 2014). In order to investigate these recent trend changes in the Southern Ocean, we also decompose the 2001–2011 trends in the Southern Ocean biomes (Table 3). In the SO-STSS biome we find no change in what drives the pH trend for this decade compared to the longer period. However, the change in the observed pH trend (Table 3) appears to be dominated by the change in DIC as this is approximately four times larger (more negative) for the period 2001–2011 than for the period 1981–2011, and therefore likely dominates over the thermally induced reduction of the pH trends. In the SO-SPSS biome we find an increase in the DIC driven pH trend within the period 2001–2011 compared to the period 1981–2011, and since the DIC component is negative this supports the conclusion drawn by Fay and McKinley (2013) that a reduction in vertical DIC support causes the weakening of both fCO_2 and pH trends in this region. In the SO-ICE biome the sign of the non-thermal drivers appears to change within the last decade, potentially driven by the recent Antarctic ice melt and ice-sheet melting driven iron fertilization (Death et al., 2014).

BGD
11, 15549–15584, 2014

3.5 Spatial variability

In both the observations and the sub-sampled model results we see significant regional differences in the pH trends (Fig. 5). Note that the actual simulated pH trends in each biome are not directly comparable with the observed trends since the model is a coupled climate model, which simulates its own internal climate variability. We therefore compare the fully sampled and the sub-sampled model results, and the fully sampled model results show much more uniform pH trends (Fig. 5). While these differences are mostly statistically indistinguishable within the uncertainties, it highlights the need for careful consideration of representativeness when comparing model-derived future changes and trends based on data. Figure 5 shows that in the SO-SPSS, EP-EQU, AEQU, and NP-STPS biomes the sub-sampled trend is within ±0.0001 of the fully-sampled pH trends, and an ANOVA analysis shows that only in the SP-STPS biome are the two model trends significantly different. Thus the trends based on the existing observational coverage are overall representative of the respective biomes, and it is unlikely to be major biases in our results due to low data density. However, the uncertainties in the long-term pH trend estimates remain too large, both in observations and model (Fig. 5) and this prohibits a mechanistic understanding the observed changes in most biomes. Improved sampling strategies are necessary to reduce these uncertainties and thereby improve our understanding of surface ocean carbon chemistry changes today and in the future.

This highlights the importance of both maintaining the observational networks already in place – like the voluntary observing ship (VOS) network in the North Atlantic (Watson et al., 2009) – and instigating new ones in less well-covered ocean regions. Of particular importance is improved data coverage in the Southern Pacific Ocean (SP-STPS) where the data density as of today it too low for a robust analysis of long term pH trends.

BGD
11, 15549–15584, 2014

4 Conclusions

Global surface ocean pH has decreased over the past 20 years by $-0.0018 \pm 0.0004\,yr^{-1}$. There are however large regional variations with trends ranging from $-0.0024\,yr^{-1}$ in the Indian Ocean (IO-STPS) biome to no significant change in the polar Southern Ocean (SO-ICE) biome. Our estimated global trend is very comparable to the trends found at time-series stations and to the global average trends in the CMIP5 models. In all biomes, the pH trend is predominantly driven by changes in DIC, implying that the surface ocean pH decline is a direct response to the increasing uptake of atmospheric CO_2. Despite this, the fCO_2 and pH trends do not exactly mirror each other, which is potentially linked to trends in the surface ocean buffer (Revelle) factor over the past decades. In some biomes this leads to smaller pH changes than expected from the fCO_2 change, while in others regions, the pH changes are larger than expected. Thus, knowledge of both the changing ocean DIC and the changing ocean buffer (Revelle) factor is important for understanding and accurately determining the changing ocean pH.

There are regional differences in the pH trends. It is likely that these are caused by spatial heterogeneity in the concurrent changes in buffer (Revelle) factor, while spatial heterogeneity in the surface ocean fCO_2 trends seems to have only a minor effect. Our comparison between fully-sampled model and sub-sampled output from the NorESM1-ME model indicates that variable data coverage only presents a problem in the South Pacific. This nicely highlights the overall success of the scientific community in creating observational networks that reduce data coverage issues. The many scientific studies arising from this effort – among many others the recent publications by Nakaoka et al. (2013), Landschützer et al. (2013, 2014), and Schuster et al. (2013) – show that we have come a long way in understanding how ocean carbon chemistry is evolving in a world perturbed by fossil fuel emissions. The uncertainties in the trends presented here are, however, substantial and this largely prevents a more thorough understanding of current changes. Filling the remaining gaps in our surface ocean data,

BGD
11, 15549–15584, 2014

Trends and drivers in global surface ocean pH over the past three decades

S. K. Lauvset et al.

and quantifying spatial patterns in the carbon chemistry parameters, is, therefore, still of great importance in order to accurately assess the open ocean carbon chemistry changes.

Acknowledgements. The work of S. K. Lauvset was funded by the Norwegian Reseach Council through the project DECApH (214513/F20). Are Olsen ackonwledge funding from the Centre for Climate Dynamics at the Bjerknes Centre for Climate Research, and the Norwegian Research Council project SNACS (229756). N. Gruber and P. Landschützer acknowledge funding from the ETH and the EU FP7 projects CARBOCHANGE (264879) and GEOCARBON (283080). J. Tjiputra acknowledges the Centre for Climate Dynamics project BIOFEEDBACK.

References

Antonov, J., Seidov, D., Boyer, T., Locarnini, R., Mishonov, A., Garcia, H., Baranova, O., Zweng, M., and Johnson, D.: World Ocean Atlas 2009, vol. 2, Salinity, edited by: Levitus, S., US Gov. Print. Off., Washington, DC, 184 pp., 2010.

Bakker, D. C. E., Pfeil, B., Smith, K., Hankin, S., Olsen, A., Alin, S. R., Cosca, C., Harasawa, S., Kozyr, A., Nojiri, Y., O'Brien, K. M., Schuster, U., Telszewski, M., Tilbrook, B., Wada, C., Akl, J., Barbero, L., Bates, N. R., Boutin, J., Bozec, Y., Cai, W.-J., Castle, R. D., Chavez, F. P., Chen, L., Chierici, M., Currie, K., de Baar, H. J. W., Evans, W., Feely, R. A., Fransson, A., Gao, Z., Hales, B., Hardman-Mountford, N. J., Hoppema, M., Huang, W.-J., Hunt, C. W., Huss, B., Ichikawa, T., Johannessen, T., Jones, E. M., Jones, S. D., Jutterström, S., Kitidis, V., Körtzinger, A., Landschützer, P., Lauvset, S. K., Lefèvre, N., Manke, A. B., Mathis, J. T., Merlivat, L., Metzl, N., Murata, A., Newberger, T., Omar, A. M., Ono, T., Park, G.-H., Paterson, K., Pierrot, D., Ríos, A. F., Sabine, C. L., Saito, S., Salisbury, J., Sarma, V. V. S. S., Schlitzer, R., Sieger, R., Skjelvan, I., Steinhoff, T., Sullivan, K. F., Sun, H., Sutton, A. J., Suzuki, T., Sweeney, C., Takahashi, T., Tjiputra, J., Tsurushima, N., van Heuven, S. M. A. C., Vandemark, D., Vlahos, P., Wallace, D. W. R., Wanninkhof, R., and Watson, A. J.: An update to the Surface Ocean CO_2 Atlas (SOCAT version 2), Earth Syst. Sci. Data, 6, 69–90, doi:10.5194/essd-6-69-2014, 2014.

Bates, N. R.: Interannual variability of the oceanic CO_2 sink in the subtropical gyre of the North Atlantic Ocean over the last 2 decades, J. Geophys. Res., 112, C09013, doi:10.1029/2006JC003759, 2007.

BGD
11, 15549–15584, 2014

Bates, N. R., Astor, Y. M., Church, M. J., Currie, K., Dore, J. E., Gonzalez-Davila, M., Lorenzoni, L., Muller-Karger, F., Olafsson, J., and Magdalena Santana-Casiano, J.: A time-series view of changing surface ocean chemistry due to ocean uptake of anthropogenic CO_2 and ocean acidification, Oceanography, 27, 126–141, 2014.
Bopp, L., Resplandy, L., Orr, J. C., Doney, S. C., Dunne, J. P., Gehlen, M., Halloran, P., Heinze, C., Ilyina, T., Séférian, R., Tjiputra, J., and Vichi, M.: Multiple stressors of ocean ecosystems in the 21st century: projections with CMIP5 models, Biogeosciences, 10, 6225–6245, doi:10.5194/bg-10-6225-2013, 2013.
Dickson, A. G. and Millero, F. J.: A comparison of the equilibrium-constants for the dissociation of carbonic-acid in seawater media, Deep-Sea Res., 34, 1733–1743, 1987.
Death, R., Wadham, J. L., Monteiro, F., Le Brocq, A. M., Tranter, M., Ridgwell, A., Dutkiewicz, S., and Raiswell, R.: Antarctic ice sheet fertilises the Southern Ocean, Biogeosciences, 11, 2635–2643, doi:10.5194/bg-11-2635-2014, 2014.
Doney, S. C., Balch, W. M., Fabry, V. J., and Feely, R. A.: Ocean acidification: a critical emerging problem for the ocean sciences, Oceanography, 22, 16–25, 2009a.
Doney, S. C., Fabry, V. J., Feely, R. A., and Kleypas, J. A.: Ocean acidification: the other CO_2 problem, Annual Review of Marine Science, 1, 169–192, 2009b.
Dore, J. E., Lukas, R., Sadler, D. W., Church, M. J., and Karl, D. M.: Physical and biogeochemical modulation of ocean acidification in the central North Pacific, P. Natl. Acad. Sci. USA, 106, 12235–12240, 2009.
Fay, A. R. and McKinley, G. A.: Global trends in surface ocean $p\mathrm{CO_2}$ from in situ data, Global Biogeochem. Cy., 27, 541–557, 2013.
Fay, A. R. and McKinley, G. A.: Global Ocean Biomes: Mean and time-varying maps (NetCDF 7.8 MB), doi:10.1594/PANGAEA.828650, 2014, Supplement to: Fay, A. R. and McKinley, G. A.: Global open-ocean biomes: mean and temporal variability, Earth Syst. Sci. Data, 6, 273–284, doi:10.5194/essd-6-273-2014, 2014.
Fay, A. R., McKinley, G. A., and Lovenduski, N. S.: Southern Ocean carbon trends: sensitivity to methods, Geophys. Res. Lett., 41, doi:10.1002/2014GL061324, online first, 2014.
Gattuso, J.-P. and Hansson, L.: Ocean Acidification, Oxford University Press, New York, 2011.
González-Dávila, M., Santana-Casiano, J. M., and González-Dávila, E. F.: Interannual variability of the upper ocean carbon cycle in the northeast Atlantic Ocean, Geophys. Res. Lett., 34, L07608, doi:10.1029/2006GL028145, 2007.

González-Dávila, M., Santana-Casiano, J. M., Rueda, M. J., and Llinás, O.: The water column distribution of carbonate system variables at the ESTOC site from 1995 to 2004, Biogeosciences, 7, 3067–3081, doi:10.5194/bg-7-3067-2010, 2010.

Landschützer, P., Gruber, N., Bakker, D. C. E., Schuster, U., Nakaoka, S., Payne, M. R., Sasse, T. P., and Zeng, J.: A neural network-based estimate of the seasonal to inter-annual variability of the Atlantic Ocean carbon sink, Biogeosciences, 10, 7793–7815, doi:10.5194/bg-10-7793-2013, 2013.

Landschützer, P., Gruber, N., Bakker, D. C. E., and Schuster, U.: Recent variability of the global ocean carbon sink, Global Biogeochem. Cy., 28, 927–949, doi:10.1002/2014GB004853, 2014.

Lauvset, S. K. and Gruber, N.: Long-term trends in surface ocean pH in the North Atlantic, Mar. Chem., 162, 71–76, 2014.

Lewis, E. and Wallace, D. W. R.: Program Developed for CO_2 System Calculations, ORNL/CDIAC-105, Carbon Dioxide Information Analysis Center, Oak Ridge National Laboratory, U.S. Department of Energy, Oak Ridge, Tennessee, 1998.

Le Quéré, C.: Trends in the land and ocean carbon uptake, Current Opinion in Environmental Sustainability, 2, 219–224, 2010.

Le Quéré, C., Peters, G. P., Andres, R. J., Andrew, R. M., Boden, T. A., Ciais, P., Friedlingstein, P., Houghton, R. A., Marland, G., Moriarty, R., Sitch, S., Tans, P., Arneth, A., Arvanitis, A., Bakker, D. C. E., Bopp, L., Canadell, J. G., Chini, L. P., Doney, S. C., Harper, A., Harris, I., House, J. I., Jain, A. K., Jones, S. D., Kato, E., Keeling, R. F., Klein Goldewijk, K., Körtzinger, A., Koven, C., Lefèvre, N., Maignan, F., Omar, A., Ono, T., Park, G.-H., Pfeil, B., Poulter, B., Raupach, M. R., Regnier, P., Rödenbeck, C., Saito, S., Schwinger, J., Segschneider, J., Stocker, B. D., Takahashi, T., Tilbrook, B., van Heuven, S., Viovy, N., Wanninkhof, R., Wiltshire, A., and Zaehle, S.: Global carbon budget 2013, Earth Syst. Sci. Data, 6, 235–263, doi:10.5194/essd-6-235-2014, 2014.

Lee, K., Tong, L. T., Millero, F. J., Sabine, C. L., Dickson, A. G., Goyet, C., Park, G.-H., Wanninkhof, R., Feely, R. A., and Key, R. M.: Global relationships of total alkalinity with salinity and temperature in surface waters of the world's oceans, Geophys. Res. Lett., 33, L19605, doi:10.1029/2006GL027207, 2006.

Lenton, A., Metzl, N., Takahashi, T., Kuchinke, M., Matear, R. J., Roy, T., Sutherland, S. C., Sweeney, C., and Tilbrook, B.: The observed evolution of oceanic $p\mathrm{CO}_2$ and its drivers over the last two decades, Global Biogeochem. Cy., 26, GB2021, doi:10.1029/2011GB004095, 2012.

McGrath, T., Kivimae, C., Tanhua, T., Cave, R. R., and McGovern, E.: Inorganic carbon and pH levels in the Rockall Trough 1991–2010, Deep-Sea Res. Pt. I, 68, 79–91, 2012.

Mehrbach, C., Culberso, C., Hawley, J. E., and Pytkowic, R.: Measurement of apparent dissociation-constants of carbonic-acid in seawater at atmospheric-pressure, Limnol. Oceanogr., 18, 897–907, 1973.

Metzl, N.: Decadal increase of oceanic carbon dioxide in Southern Indian Ocean surface waters (1991–2007), Deep-Sea Res. Pt. II, 56, 607–619, 2009.

Nakaoka, S., Telszewski, M., Nojiri, Y., Yasunaka, S., Miyazaki, C., Mukai, H., and Usui, N.: Estimating temporal and spatial variation of ocean surface $p\mathrm{CO_2}$ in the North Pacific using a self-organizing map neural network technique, Biogeosciences, 10, 6093–6106, doi:10.5194/bg-10-6093-2013, 2013.

Nondal, G., Bellerby, R. G. J., Olsen, A., Johannessen, T., and Olafsson, J.: Optimal evaluation of the surface ocean CO_2 system in the northern North Atlantic using data from voluntary observing ships, Limnol. Oceanogr.-Meth., 7, 109–118, 2009.

Olafsson, J., Olafsdottir, S. R., Benoit-Cattin, A., and Takahashi, T.: The Irminger Sea and the Iceland Sea time series measurements of sea water carbon and nutrient chemistry 1983–2008, Earth Syst. Sci. Data, 2, 99–104, doi:10.5194/essd-2-99-2010, 2010.

Orr, J.: Recent and future changes in ocean carbonate chemistry, in: Ocean Acidification, edited by: Gattuso, J.-P. and Hansson, L., Oxford University Press, New York, 41–66, 2011.

Pfeil, B., Olsen, A., Bakker, D. C. E., Hankin, S., Koyuk, H., Kozyr, A., Malczyk, J., Manke, A., Metzl, N., Sabine, C. L., Akl, J., Alin, S. R., Bates, N., Bellerby, R. G. J., Borges, A., Boutin, J., Brown, P. J., Cai, W.-J., Chavez, F. P., Chen, A., Cosca, C., Fassbender, A. J., Feely, R. A., González-Dávila, M., Goyet, C., Hales, B., Hardman-Mountford, N., Heinze, C., Hood, M., Hoppema, M., Hunt, C. W., Hydes, D., Ishii, M., Johannessen, T., Jones, S. D., Key, R. M., Körtzinger, A., Landschützer, P., Lauvset, S. K., Lefèvre, N., Lenton, A., Lourantou, A., Merlivat, L., Midorikawa, T., Mintrop, L., Miyazaki, C., Murata, A., Nakadate, A., Nakano, Y., Nakaoka, S., Nojiri, Y., Omar, A. M., Padin, X. A., Park, G.-H., Paterson, K., Perez, F. F., Pierrot, D., Poisson, A., Ríos, A. F., Santana-Casiano, J. M., Salisbury, J., Sarma, V. V. S. S., Schlitzer, R., Schneider, B., Schuster, U., Sieger, R., Skjelvan, I., Steinhoff, T., Suzuki, T., Takahashi, T., Tedesco, K., Telszewski, M., Thomas, H., Tilbrook, B., Tjiputra, J., Vandemark, D., Veness, T., Wanninkhof, R., Watson, A. J., Weiss, R., Wong, C. S., and Yoshikawa-Inoue, H.: A uniform, quality controlled Surface Ocean CO_2 Atlas (SOCAT), Earth Syst. Sci. Data, 5, 125–143, doi:10.5194/essd-5-125-2013, 2013.

Rödenbeck, C., Bakker, D. C. E., Metzl, N., Olsen, A., Sabine, C., Cassar, N., Reum, F., Keeling, R. F., and Heimann, M.: Interannual sea–air CO_2 flux variability from an observation-driven ocean mixed-layer scheme, Biogeosciences, 11, 4599–4613, doi:10.5194/bg-11-4599-2014, 2014.

Sarmiento, J. L. and Gruber, N.: Ocean Biogeochemical Dynamics, Princeton University Press, Princeton, NJ, 2006.

Schuster, U., McKinley, G. A., Bates, N., Chevallier, F., Doney, S. C., Fay, A. R., González-Dávila, M., Gruber, N., Jones, S., Krijnen, J., Landschützer, P., Lefèvre, N., Manizza, M., Mathis, J., Metzl, N., Olsen, A., Rios, A. F., Rödenbeck, C., Santana-Casiano, J. M., Takahashi, T., Wanninkhof, R., and Watson, A. J.: An assessment of the Atlantic and Arctic sea–air CO_2 fluxes, 1990–2009, Biogeosciences, 10, 607–627, doi:10.5194/bg-10-607-2013, 2013.

Steinacher, M., Joos, F., Frölicher, T. L., Plattner, G.-K., and Doney, S. C.: Imminent ocean acidification in the Arctic projected with the NCAR global coupled carbon cycle-climate model, Biogeosciences, 6, 515–533, doi:10.5194/bg-6-515-2009, 2009.

Takahashi, T., Olafsson, J., Goddard, J. G., Chipman, D. W., and Sutherland, S. C.: Seasonal-variation of CO_2 and nutrients in the high-latitude surface oceans – a comparative study, Global Biogeochem. Cy., 7, 843–878, 1993.

Takahashi, T., Sutherland, S. C., Sweeney, C., Poisson, A., Metzl, N., Tilbrook, B., Bates, N. R., Wanninkhof, R., Feely, R. A., Sabine, C. L., Olafsson, J., and Nojiri, Y.: Global sea–air CO_2 flux based on climatological surface ocean $p$$CO_2$, and seasonal biological and temperature effects, Deep-Sea Res. Pt. II, 49, 1601–1622, 2002.

Takahashi, T., Sutherland, S. C., and Kozyr, A.: Global Ocean Surface Water Partial Pressure of CO_2 Database: Measurements Performed During 1968–2008 (Version 2008), ORNL/CDIAC-152, NDP-088r, Carbon Dioxide Information Analysis Center, Oak Ridge National Laboratory, U.S. Department of Energy, Oak Ridge, Tennessee, 2009a.

Takahashi, T., Sutherland, S. C., Wanninkhof, R., Sweeney, C., Feely, R. A., Chipman, D. W., Hales, B., Friederich, G., Chavez, F., Sabine, C., Watson, A., Bakker, D. C. E., Schuster, U., Metzl, N., Yoshikawa-Inoue, H., Ishii, M., Midorikawa, T., Nojiri, Y., Körtzinger, A., Steinhoff, T., Hoppema, M., Olafsson, J., Arnarson, T. S., Tilbrook, B., Johannessen, T., Olsen, A., Bellerby, R., Wong, C. S., Delille, B., Bates, N. R., and de Baar, H. J. W.: Climatological

BGD

11, 15549–15584, 2014

mean and decadal change in surface ocean pCO_2, and net sea–air CO_2 flux over the global oceans, Deep-Sea Res. Pt. II, 56, 554–577, 2009b.

Takahashi, T., Sutherland, S. C., Chipman, D. W., Goddard, J. G., Ho, C., Newberger, T., Sweeney, C., and Munro, D. R.: Climatological distributions of pH, pCO_2, total CO_2, alkalinity, and $CaCO_3$ saturation in the global surface ocean, and temporal changes at selected locations, Mar. Chem., 164, 95–125, 2014.

Taylor, K. E., Stouffer, R. J., and Meehl, G. A.: An overview of CMIP5 and the experiment design, B. Am. Meteorol. Soc., 93, 485–498, 2012.

Tjiputra, J. F., Roelandt, C., Bentsen, M., Lawrence, D. M., Lorentzen, T., Schwinger, J., Seland, Ø., and Heinze, C.: Evaluation of the carbon cycle components in the Norwegian Earth System Model (NorESM), Geosci. Model Dev., 6, 301–325, doi:10.5194/gmd-6-301-2013, 2013.

Tjiputra, J. F., Olsen, A. R. E., Bopp, L., Lenton, A., Pfeil, B., Roy, T., Segschneider, J., Totterdell, I. A. N., and Heinze, C.: Long-term surface pCO_2 trends from observations and models, Tellus B, 66, 23083, doi:10.3402/tellusb.v66.23083, 2014.

Uppstrom, L. R.: Boron/chlorinity ratio of deep-sea water from pacific ocea, Deep-Sea Res., 21, 161–162, 1974.

Vijayvargiya, A.: One-way analysis of variance, Journal of Validation Technology, 15, 62–63, 2009.

Watson, A. J., Schuster, U., Bakker, D. C. E., Bates, N. R., Corbiere, A., Gonzalez-Davila, M., Friedrich, T., Hauck, J., Heinze, C., Johannessen, T., Körtzinger, A., Metzl, N., Olafsson, J., Olsen, A., Oschlies, A., Padin, X. A., Pfeil, B., Santana-Casiano, J. M., Steinhoff, T., Telszewski, M., Rios, A. F., Wallace, D. W. R., and Wanninkhof, R.: Tracking the variable North Atlantic sink for atmospheric CO_2, Science, 326, 1391–1393, 2009.

Zeebe, R. E. and Wolf-Gladrow, D.: CO_2 in Seawater, Equilibrium, Kinetics, Isotopes, Elsevier, Amsterdam, Pays-Bas, 2001.

BGD
11, 15549–15584, 2014
Trends and drivers in global surface ocean pH over the past three decades
S. K. Lauvset et al.

Table 1. Results and statistics of the regression analysis of fCO_2 and pH_{insitu} vs. time. Bold text indicates biomes where the results are not statistically significant (95 % confidence). No number is given if a biome does not have enough data to calculate the trend in a given time period.

Region	1981–2011				1991–2011			
	pH		fCO_2		pH		fCO_2	
	slope	rmse	slope	rmse	slope	rmse	slope	rmse
NP-SPSS	**−0.0003 ± 0.0005**	**0.041**	1.29 ± 0.17	16.2	0.0013 ± 0.0005	0.038	0.78 ± 0.22	16.1
NP-STSS	–	–	1.36 ± 0.09	10.5	−0.0010 ± 0.0005	0.031	1.54 ± 0.10	8.9
NP-STPS	−0.0016 ± 0.0002	0.020	1.45 ± 0.08	10.3	−0.0019 ± 0.0002	0.018	1.57 ± 0.11	9.9
WP-EQU	−0.0010 ± 0.0002	0.016	1.27 ± 0.15	17.8	−0.0012 ± 0.0002	0.015	1.57 ± 0.23	17.3
EP-EQU	−0.0023 ± 0.0003	0.023	2.56 ± 0.36	28.2	−0.0026 ± 0.0002	0.023	3.33 ± 0.46	27.9
SP-STPS	−0.0019 ± 0.0002	0.020	1.32 ± 0.11	12.0	−0.0022 ± 0.0003	0.020	1.15 ± 0.16	12.3
NA-SPSS	–	–	1.18 ± 0.16	15.4	−0.0020 ± 0.0004	0.028	1.11 ± 0.19	14.2
NA-STSS	–	–	1.78 ± 0.14	12.3	−0.0018 ± 0.0003	0.015	1.78 ± 0.16	12.5
NA-STPS	–	–	1.46 ± 0.09	8.5	−0.0011 ± 0.0002	0.012	1.51 ± 0.11	8.6
A-EQU	–	–	1.62 ± 0.25	16.6	−0.0016 ± 0.0003	0.014	1.76 ± 0.31	15.7
SA-STPS	–	–	0.95 ± 0.21	16.7	−0.0011 ± 0.0005	0.024	0.82 ± 0.31	17.0
IO-STPS	−0.0024 ± 0.0004	0.023	1.44 ± 0.24	13.6	−0.0027 ± 0.0005	0.025	1.56 ± 0.26	13.5
SO-STSS	**−0.0006 ± 0.0004**	**0.032**	1.77 ± 0.1	10.8	**−0.0004 ± 0.0004**	**0.032**	1.91 ± 0.12	10.8
SO-SPSS	−0.0020 ± 0.0002	0.020	1.40 ± 0.09	9.1	−0.0021 ± 0.0002	0.020	1.45 ± 0.11	9.0
SO-ICE	–	–	0.70 ± 0.28	24.4	**−0.0002 ± 0.0004**	**0.029**	0.25 ± 0.33	24.3

BGD
11, 15549–15584, 2014
Trends and drivers in global surface ocean pH over the past three decades
S. K. Lauvset et al.

Table 2. Decomposition of the fCO_2 and pH_{insitu} trends into their major drivers.

Region	pH					fCO_2				
	theta	salinity	DIC	alkalinity	sum	theta	salinity	DIC	alkalinity	sum
NP-SPSS	−0.57	−0.15	3.18	−3.04	−0.58	0.52	0.14	−2.89	2.76	0.53
NP-STSS	−0.39	0.02	−0.89	−0.13	−1.39	0.38	−0.02	0.87	0.13	1.37
NP-STPS	1.15	−0.02	−1.68	0.04	−0.50	−1.19	0.02	1.73	−0.05	0.51
WP-EQU	−0.47	0.11	−0.87	0.14	−1.10	0.53	−0.12	0.97	−0.15	1.23
EP-EQU	0.51	−0.07	−2.99	0.13	−2.42	−0.63	0.08	3.68	−0.15	2.99
SP-STPS	2.28	−0.11	−3.02	0.04	−0.81	−2.47	0.12	3.28	−0.05	0.88
NA-SPSS	−0.02	0.17	−2.41	0.12	−2.13	0.01	−0.16	2.17	−0.11	1.91
NA-STSS	0.74	−0.07	−1.43	−0.11	−0.87	−0.72	0.07	1.40	0.10	0.85
NA-STPS	−1.20	−0.05	−0.10	−0.12	−1.47	1.29	0.05	0.11	0.13	1.57
A-EQU	−0.21	0.02	−1.33	−0.05	−1.56	0.24	−0.03	1.53	0.06	1.80
SA-STPS	−0.31	0.06	−1.55	−0.05	−1.85	0.34	−0.07	1.69	0.05	2.02
IO-STPS	0.80	−0.02	−3.23	0.06	−2.39	−0.79	0.02	3.22	−0.06	2.38
SO-STSS	−0.99	−0.08	2.02	−0.86	0.09	0.88	0.08	−1.81	0.77	−0.08
SO-SPSS	0.89	0.01	−3.09	0.53	−1.66	−0.83	−0.01	2.89	−0.50	1.56
SO-ICE	0.13	−0.01	−2.22	0.15	−1.95	−0.12	0.01	2.02	−0.13	1.78

Table 3. Decomposition of the 2001–2011 fCO_2 and pH_{insitu} trends in the Southern Ocean into their major drivers.

Region	pH						fCO_2					
	theta	salinity	DIC	alkalinity	sum	observed	theta	salinity	DIC	alkalinity	sum	observed
SO-STSS	−3.7	−0.79	8.46	−2.48	1.49	0.0032 ± 0.0010	3.4	0.73	−7.78	2.28	−1.37	1.56 ± 0.39
SO-SPSS	1.11	−0.07	−1.28	−0.05	−0.29	−0.0011 ± 0.0006	−1.06	0.07	1.22	0.05	0.28	0.89 ± 0.22
SO-ICE	−0.62	−0.05	1.00	−0.39	−0.06	0.0006 ± 0.0009	0.59	0.05	−0.95	0.37	0.06	0.21 ± 0.74

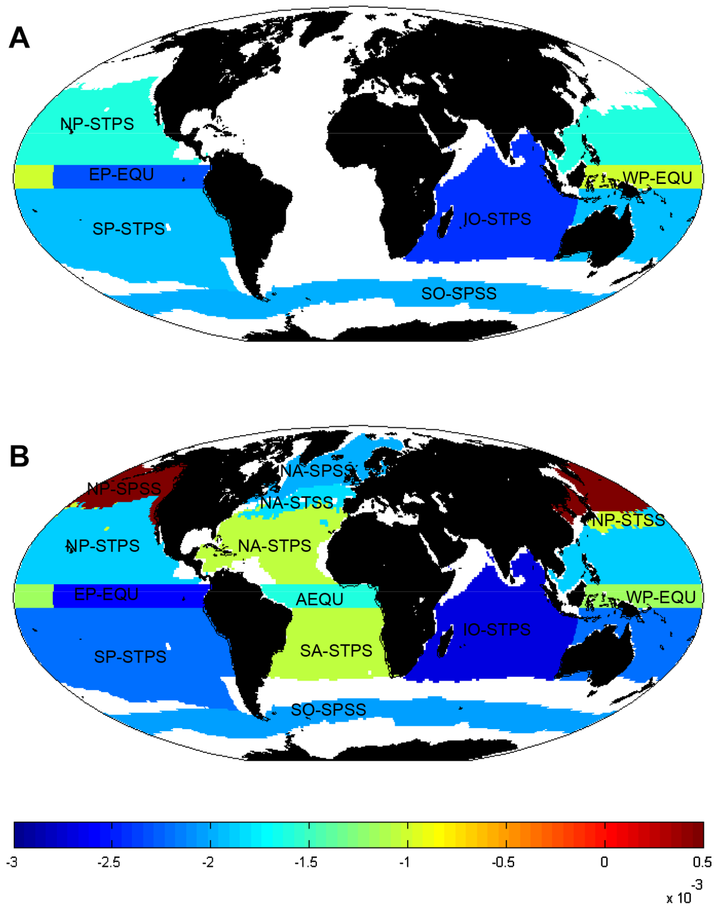

Figure 1. A map of the Fay and McKinley (2014) biomes which have **(a)** a statistically significant pH trend in the period 1981–2011, and **(b)** the biomes with a statistically significant pH trend in the period 1991–2011.

BGD
11, 15549–15584, 2014

Trends and drivers in global surface ocean pH over the past three decades

S. K. Lauvset et al.

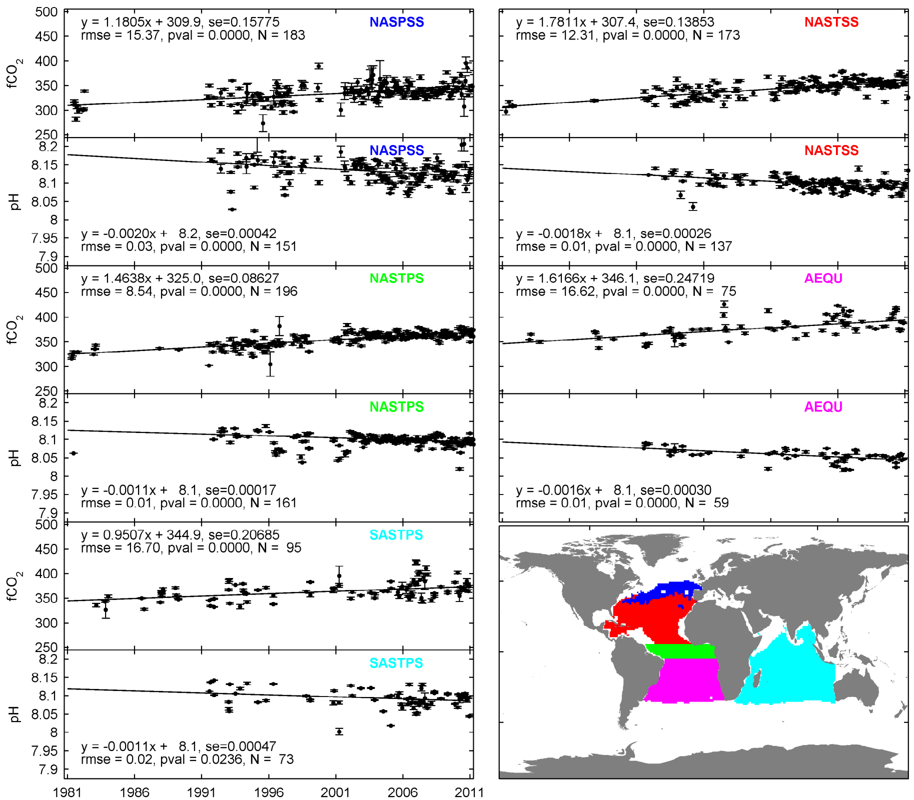

Figure 2. Long term fCO_2 and pH trend (1981–2011) in the five Atlantic Ocean biomes.

BGD
11, 15549–15584, 2014

Trends and drivers in global surface ocean pH over the past three decades

S. K. Lauvset et al.

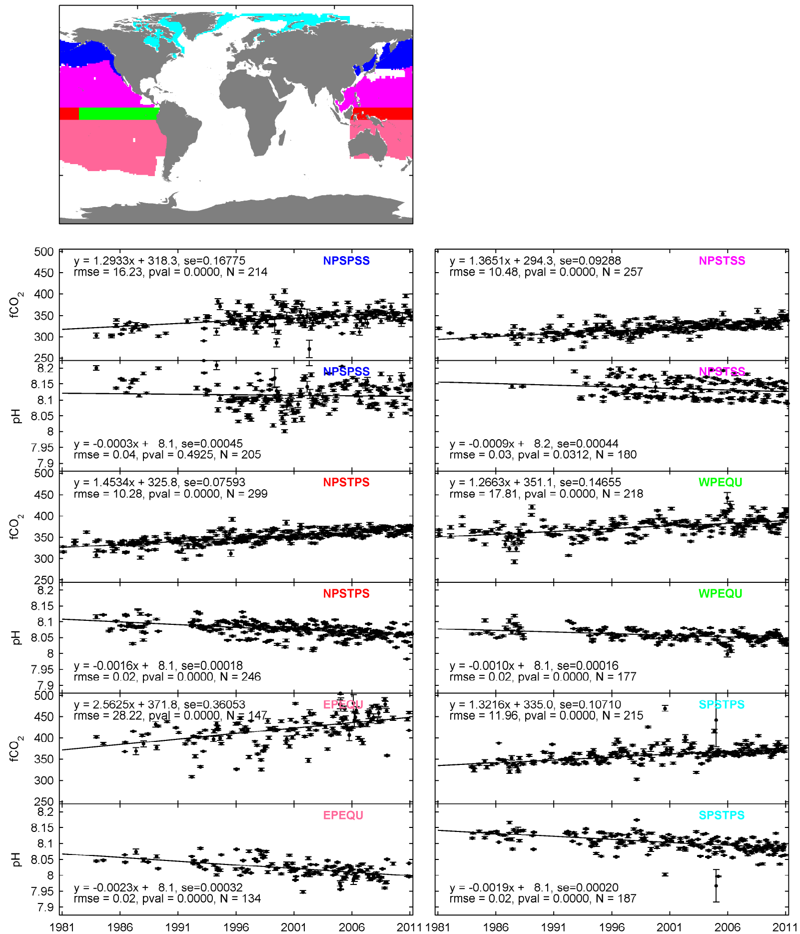

Figure 3. Long term pH trend (1981–2011) in the five Pacific Ocean biomes.

BGD
11, 15549–15584, 2014

Trends and drivers in global surface ocean pH over the past three decades

S. K. Lauvset et al.

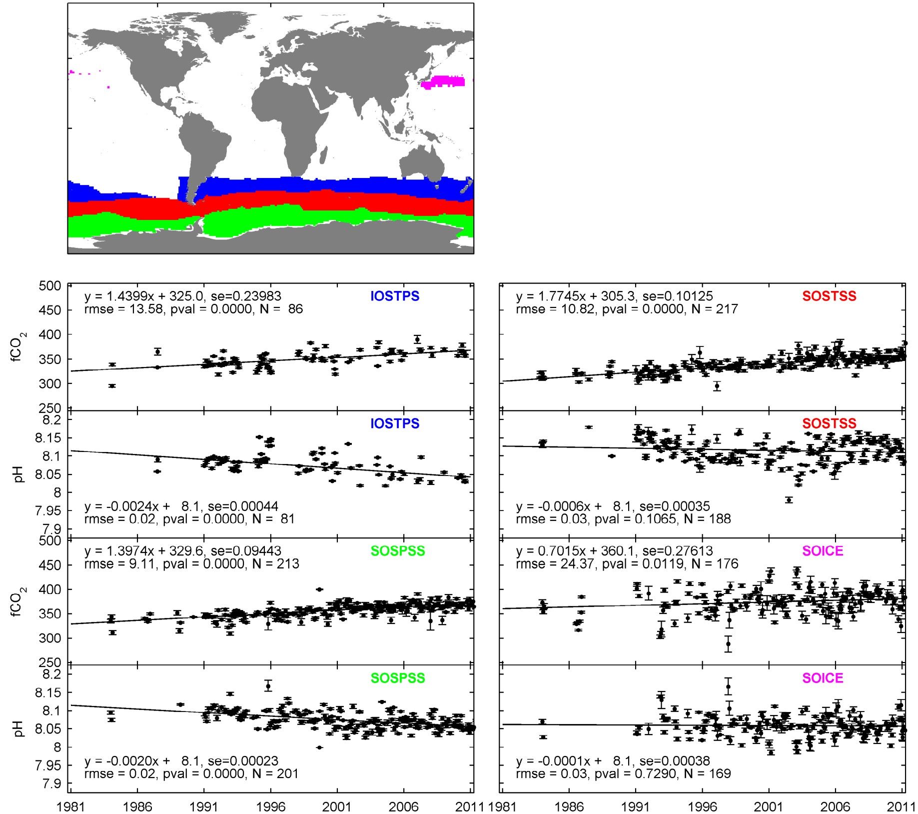

Figure 4. Long term pH trend (1981–2011) in the Indian Ocean biome and the three Southern Ocean biomes.

BGD
11, 15549–15584, 2014

Trends and drivers in global surface ocean pH over the past three decades

S. K. Lauvset et al.

Title Page
Abstract | Introduction
Conclusions | References
Tables | Figures
◄ | ►
◄ | ►
Back | Close
Full Screen / Esc
Printer-friendly Version
Interactive Discussion

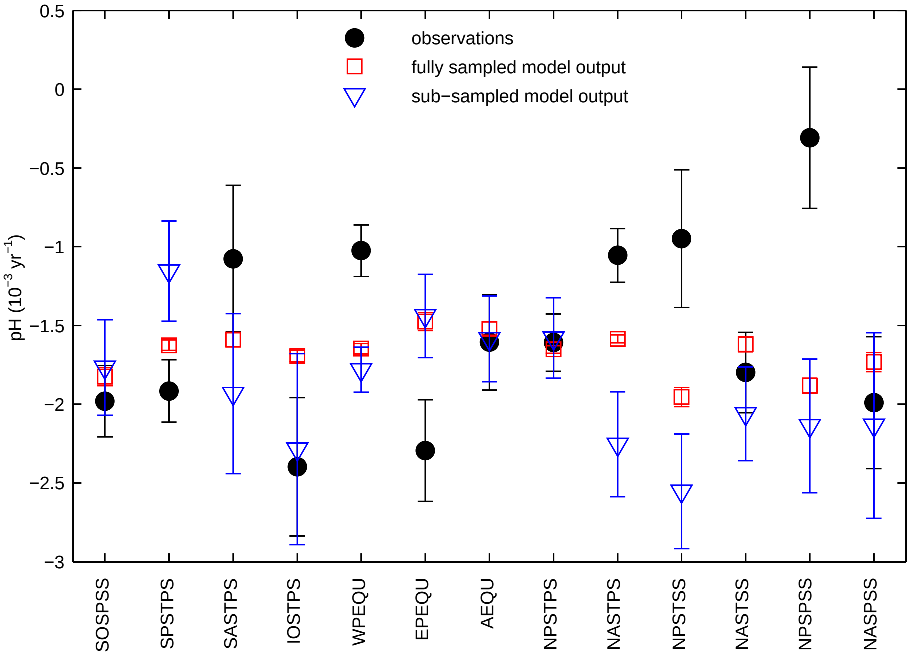

Figure 5. Summary of the pH trends in all biomes. The error bars show the 1σ confidence interval.

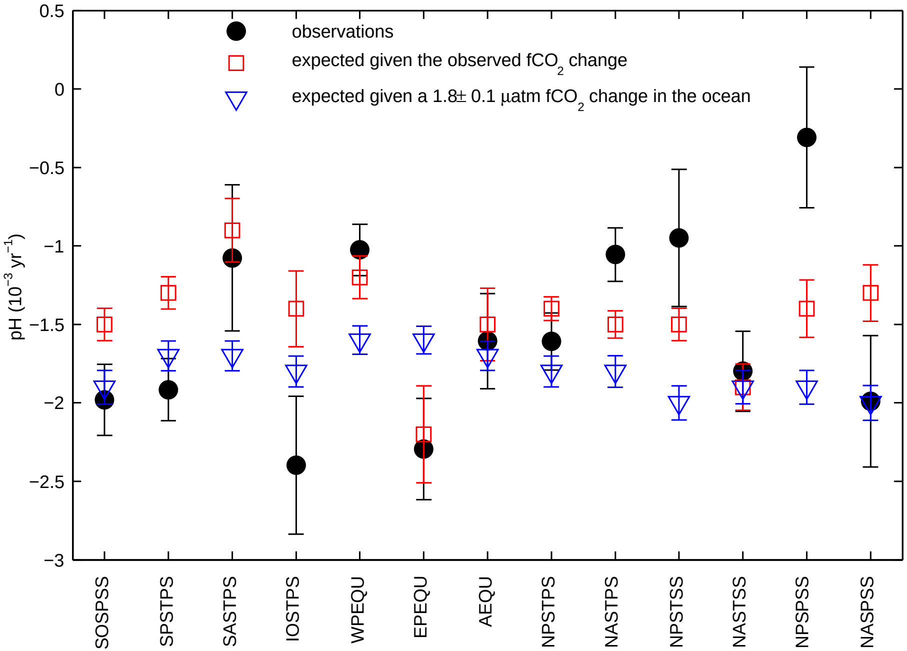

Figure 6. Comparison between the observed pH trend in each biome (either 1981–2011 or 1991–2011) in black and the pH trends expected if the surface ocean fCO_2 changed equal to the atmosphere (blue) and expected for the observed ocean fCO_2 trends (red).

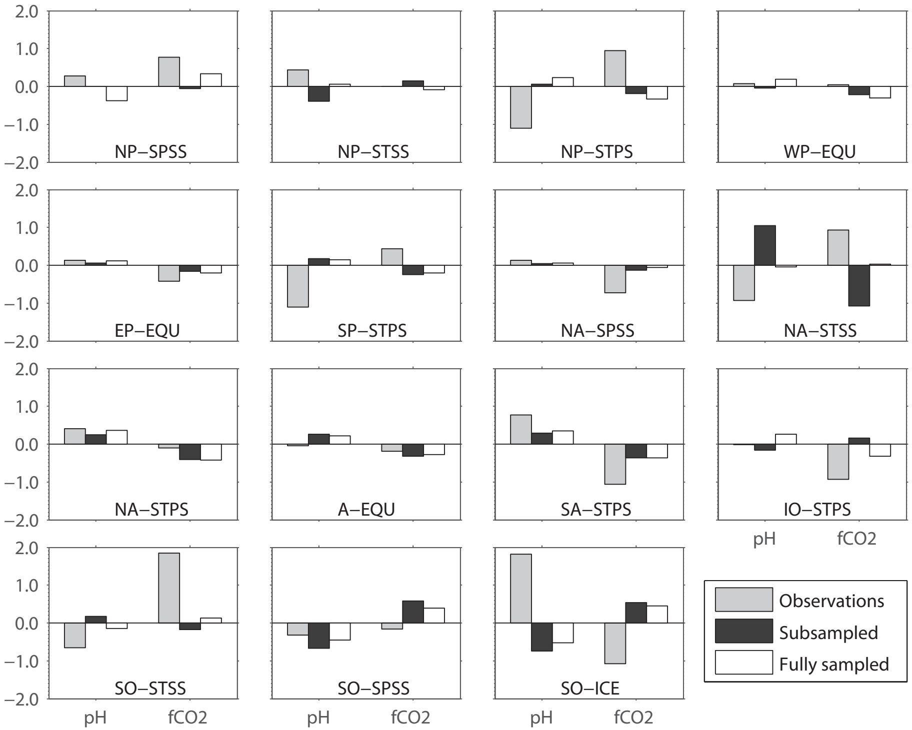

Figure 7. The residual between the actual trends in pH and fCO_2 and the sum of the four decomposition parts (SSS, SST, DIC, ALK). In gray is the residual for the observations, in black the residual for the sub-sampled model output, and in white the residual for the fully-sampled model output.

BGD
11, 15549–15584, 2014

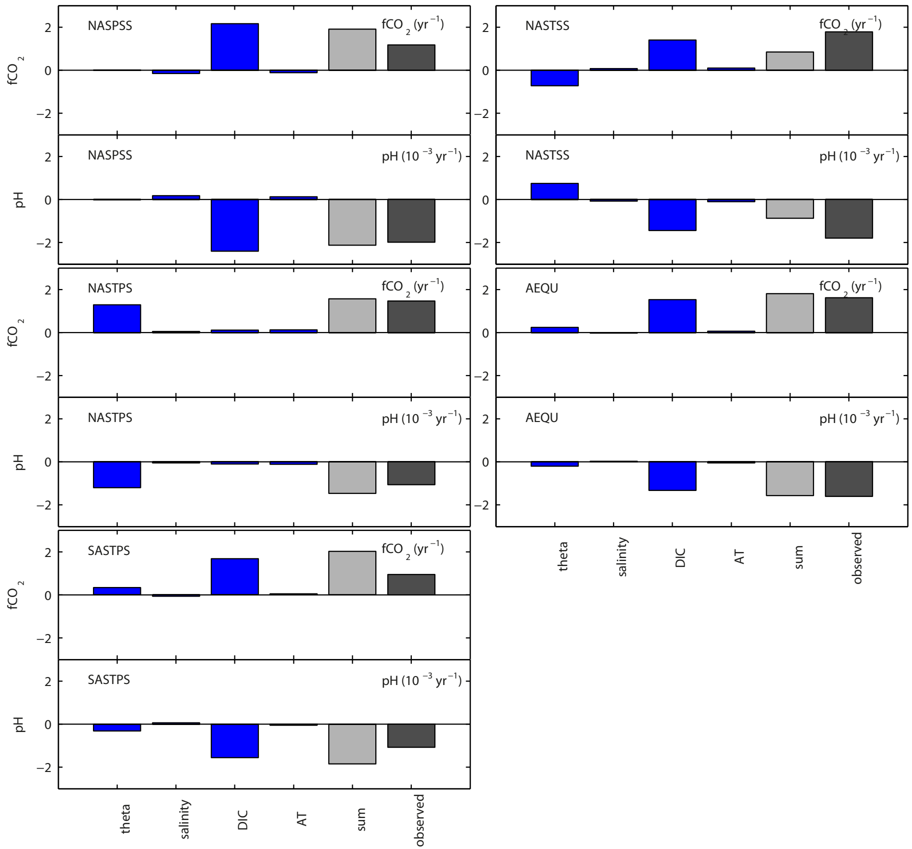

Figure 8. The long term trends in fCO_2 and pH from Fig. 2 decomposed into the contributions from SST, SSS, alkalinity, and DIC. Also shown is the sum of the four contributions and the actual observed trend. Note that for pH the trend has been multiplied by 1000 for easier visualization.

BGD

11, 15549–15584, 2014

Trends and drivers in global surface ocean pH over the past three decades

S. K. Lauvset et al.

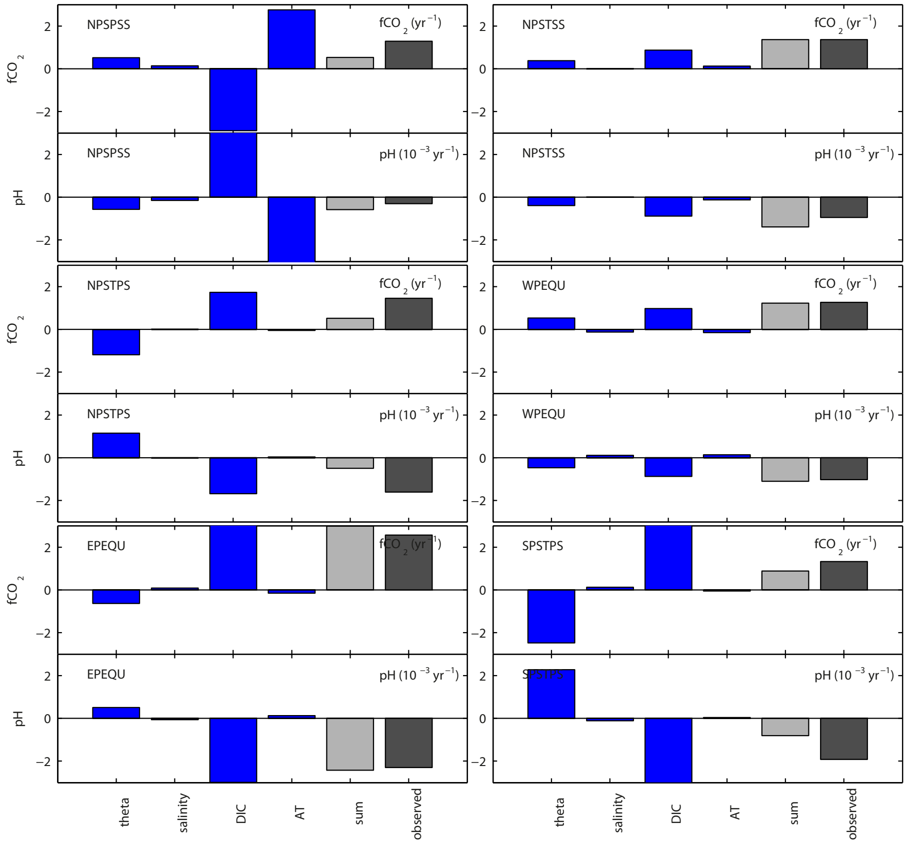

Figure 9. The long term trends in fCO_2 and pH from Fig. 3 decomposed into the contributions from SST, SSS, alkalinity, and DIC. Also shown is the sum of the four contributions and the actual observed trend. Note that for pH the trend has been multiplied by 1000 for easier visualization.

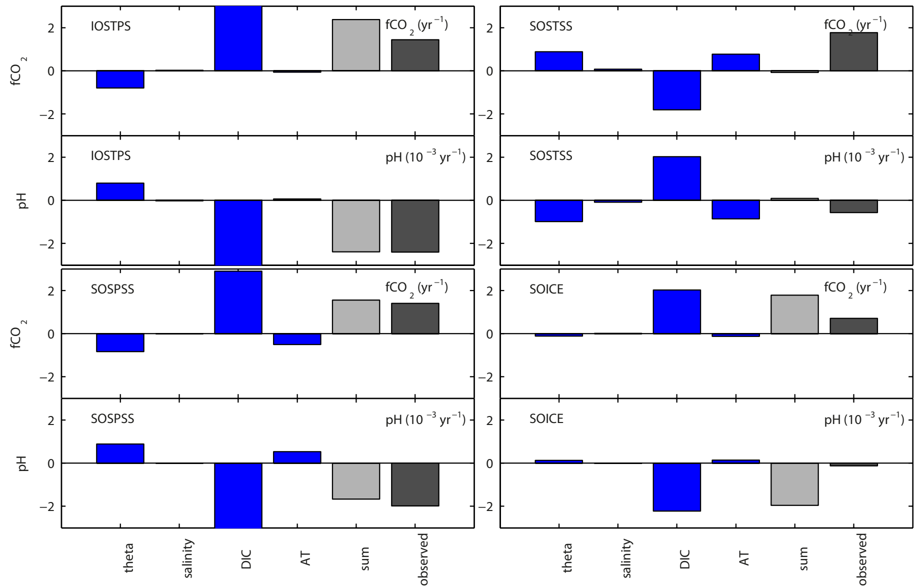

Figure 10. The long term trends in fCO_2 and pH from Fig. 4 decomposed into the contributions from SST, SSS, alkalinity, and DIC. Also shown is the sum of the four contributions and the actual observed trend. Note that for pH the trend has been multiplied by 1000 for easier visualization.

BGD
11, 15549–15584, 2014

Trends and drivers in global surface ocean pH over the past three decades

S. K. Lauvset et al.